

Perinatal changes in fetal cardiac geometry and function in gestational diabetic pregnancies at term

Dr Olga Patey MD PhD*†‡, Professor Julene S Carvalho MD PhD*†‡§ and Professor Basky

Thilaganathan MD PhD*†§

Molecular & Clinical Sciences Research Institute, St George's University of London*;

Fetal Medicine Unit, St. George's University Hospitals NHS Foundation Trust, London†;

Brompton Centre for Fetal Cardiology, Royal Brompton Hospital, London‡;

Joint last authors§

Corresponding Author: Dr Olga Patey

Address: Fetal Medicine Unit

4th Floor, Lanesborough Wing

St. George's University Hospitals NHS Foundation Trust

London SW17 0QT

Email: pateyolga@gmail.com

Running Head: Perinatal fetal cardiac dysfunction in GDM

Keywords: fetal echocardiography; fetal heart; gestational diabetes mellitus; fetal hypoxemia; speckle tracking; tissue Doppler imaging; left ventricular torsion.

This article has been accepted for publication and undergone full peer review but has not been through the copyediting, typesetting, pagination and proofreading process, which may lead to differences between this version and the Version of Record. Please cite this article as doi: 10.1002/uog.20187

ABSTRACT

Objective To evaluate the effect of gestational diabetes mellitus (GDM) on fetal and neonatal cardiac geometry and function around the time of birth.

Methods A prospective study of 75 pregnant women delivering at term, comprising of 54 normal pregnancies and 21 with a diagnosis GDM. Fetal and neonatal conventional cardiac indices, spectral tissue Doppler and 2D speckle tracking imaging were performed a few days before and within hours of birth.

Results Compared to normal pregnancy, GDM fetuses demonstrated significant impairment in ventricular geometry, myocardial deformation and cardiac function (right ventricular [RV] sphericity index: 0.56 vs 0.65, LV torsion: 2.1deg/cm vs 5.6deg/cm, LV isovolumetric relaxation time': 101ms vs 115ms, and RV isovolumetric contraction time': 107ms vs 119ms, $p<0.001$ for all). When compared to normal newborns, GDM neonates revealed persistent alteration in cardiac parameters (RV sphericity index 0.43 vs 0.55, LV torsion 1.3deg/cm vs 2.8deg/cm, LV myocardial performance index [MPI'] 0.39 vs 0.51, RV MPI' 0.34 vs 0.40, $p<0.001$ for all). Paired comparison of fetal and neonatal cardiac indices in GDM demonstrated that birth resulted in significant improvement in some, but not all cardiac indices (RV sphericity index: 0.65 vs 0.55, LV torsion 5.6cm/deg vs 2.8cm/deg, RV MPI': fetus 0.50 vs neonate 0.40, $p<0.001$ for all).

Conclusions Compared to normal pregnancy, GDM term fetuses and neonates exhibit cardiac indices indicative of myocardial impairment reflecting a response to a relatively hyperglycaemic intrauterine environment with alteration in fetal loading conditions (LV preload deprivation and increased RV afterload) and adaptation to subsequent acute changes in haemodynamic load at birth. Elucidating mechanisms that contribute to the alterations in perinatal cardiac function in GDM could help in refining management and evolve better therapeutic strategies to reduce the risk of adverse pregnancy outcome.

INTRODUCTION

Diabetic pregnancy is an important cause of perinatal morbidity and mortality with a five-fold greater risk of stillbirth, with 50% of stillbirths classified as unexplained (1). The effects of maternal diabetes on the fetus are summarised by the 'Pedersen hypothesis', which postulates that maternal hyperglycaemia over-stimulates fetal pancreatic beta-cells with resultant fetal hyperinsulinemia, increased metabolic rate and a tendency to fetal hypoxemia (2). The fetal heart is one of the major organs affected by hyperinsulinemia and hypoxia, with myocardial hypertrophy extensively reported in fetuses and neonates of diabetic mothers (3, 4). Infants of diabetic mothers are also at increased risk of cardiovascular morbidity and mortality in later life (5), presumably through mechanisms that affect myocardial fibre architecture influencing cardiac geometry, myocardial deformation, and ventricular function. Conventional echo studies have found evidence of diastolic dysfunction and increased systolic contractility in gestational diabetes mellitus (GDM) fetal and neonatal groups (3, 4). However, modern cardiac imaging modalities, such as tissue Doppler and speckle tracking have fundamentally changed the way echocardiography can characterise global and regional myocardial function, demonstrated a higher sensitivity for detecting even mild myocardial damage and established a stronger predictive value for subsequent cardiovascular complications compared to conventional echo indices (6, 7). Fetal and neonatal GDM data using these novel echo modalities are limited and have produced conflicting results (8-12). No prospective data exploring fetal perinatal cardiac adaptation in GDM and persistence of cardiac dysfunction from fetal life into infancy. The aim of this study was to examine the effect of maternal diabetes at term on fetal and neonatal cardiac geometry, myocardial deformation and LV torsion.

SUBJECTS AND METHODS

Study population

This was a prospective longitudinal study of pregnancies at term including pregnancies with normal outcome (n=54) and those affected by gestational and pre-gestational diabetes mellitus (n=21). Pregnant women attending for routine antenatal care in the Fetal Medicine Unit at St. George's University Hospital between February 2014 and June 2016 were recruited if the fetuses had normal cardiac anatomy and there was no maternal or pregnancy-related co-morbidity other than diabetes. Out of 21 GDM patients, seven women had pre-gestational insulin-controlled diabetes and 14 women had gestational diabetes treated by metformin. All women in our study had appropriate control of glucose levels at the time of the fetal scan conforming to National Institute for Health and Care Excellence (NICE, 2015) guidance (13). Exclusion criteria were fetal structural and chromosomal abnormalities, adverse pregnancy outcome and pregnant women in labour. All participants gave written informed consents for fetal and neonatal cardiac assessment. The Ethics Committee of NRES Committee London-Surrey Borders approved the study protocol (Reference -12/LO/0945).

Echocardiography

Fetal B-mode, M-mode, spectral pulsed-wave (PW) Doppler, spectral tissue Doppler imaging (PW-TDI) and speckle tracking imaging (STI) echocardiograms were performed few days before birth. The neonatal cardiac assessment was conducted within hours of birth. One investigator (OP) performed all fetal and neonatal ultrasound examinations using a Vivid E9 ultrasound system (General Electric, Norway). Fetal M-mode, B-mode, and PW Doppler measurements were made with the convex array obstetric transducer 4C, while the paediatric/neonatal cardiac sector probe 12S was used for neonatal heart examination. PW-TDI curves

and 2D images for STI analysis were obtained and recorded in the same manner and with the same ultrasound transducer (adult linear transducer M5S) in both fetal and neonatal groups. *M-mode ultrasound* was used for assessment of cardiac geometry and function and ventricular longitudinal axis annular motion. *B-mode imaging* was performed for obtaining measurements of the ventricular valve and chamber dimensions and calculation of ventricular sphericity index (sphericity index= ventricular end-diastolic dimension/end-diastolic length). Relative wall thickness of the ventricles and interventricular septum was estimated as twice free wall thickness/septum divided by ventricular end-diastolic diameter (14). *PW Doppler technique* with angle correction was used to obtain Doppler signals from the inflow and outflow tracts for evaluation of diastolic and systolic function respectively and calculation of stroke volume (SV) and cardiac output (CO). *PW-TDI technique* was applied to derive cardiac indices of myocardial motion in systole and diastole, and it was also used for estimation of LV and right ventricular (RV) MPI'. *Speckle tracking imaging (STI)* was used to derive global and regional myocardial deformation indices (longitudinal, circumferential, radial and rotational) with a frame rate greater than 100 frames per second (fps). All echocardiographic measurements were performed in a single beat according to the standardised protocol of the study and with regards to previously described fetal echo techniques (15). Several digital clips were obtained, serially numbered and *anonymised* patient data was transferred to the dedicated software EchoPAC (version 112, GE Medical System) for further analysis. LV net twist was calculated by subtracting the peak basal rotation from the peak apical rotation. LV torsion was considered as a result of net twist divided by the LV end-diastolic length. The software produced the LV torsion curves only if the frame rate of short axis images was the same at LV basal and apical levels. Care was taken to correctly identify the direction of the fetal LV rotation at LV short axis basal and apical levels to ensure that interpretation of the LV direction was corrected for varied fetal

orientation according to the proposed study. The time-interval values were adjusted by cardiac cycle length normalising for the difference in heart rate. The other fetal and neonatal indices were normalised by ventricular length or end-diastolic dimension according to the study methodology (Supplemental data) and as we previously published (16).

Intra- and inter-observer reproducibility

The same observer (OP) repeated TDI and STI measurements of 25 fetal and 25 neonatal echoes in a different cardiac cycle of GE Vivid E9 ultrasound system (for TDI indices) and vendor-specific EchoPAC software (for STI indices). In randomly chosen ten fetal and ten neonatal echocardiograms, two different observers (MB and VDZ) repeated TDI and STI measurements in a different cardiac cycle (blinded to each other's measurements). Both, limits of agreement (LoA) with Bland-Altman graphs/Pitman's test of difference in variance, and intra-class correlation coefficient (ICC) were calculated.

Statistical analysis

Sample size and power calculations were performed based on our pilot data (15). Statistical analysis was performed using SPSS version 22.0 (SPSS Inc., Chicago, IL, USA). Both the Shapiro-Wilk test and Kolmogorov-Smirnov test were performed to assess the data distribution normality. If $p > 0.05$, the data distribution was considered to be normal. Besides, skewness was examined to determine the normality of the distribution. For normally distributed data, paired T-test for fetal and neonatal data comparison within GDM group, and independent samples T-test to compare fetal and neonatal cardiac geometry and function variables between two study groups (normal vs GDM) were performed. For skewed data, nonparametric Wilcoxon sign rank test for paired and Mann-Whitney test for unpaired comparisons were conducted. The differences between groups were deemed as significant only if the two-tailed p-values were less than 0.01 (Bonferroni correction for type 1 error or false positive results of multiple measurements). Additionally, linear regression analysis was used to examine the relationship between LV rotational parameters and fetal/neonatal selected cardiac indices.

RESULTS

A total of 75 women consented to participate in the study (54 normal and 21 GDM pregnancies). Deformational data in basal/apical four chamber views were obtained in 73 fetuses and 66 neonates, and short axis views were in 47 fetuses and 54 neonates because of challenging image acquisition in late gestation and loss of follow-up, respectively. The 2D speckle tracking analysis was possible in all acquired images. Demographic characteristics and scan details of the pregnancies enrolled in the study are summarised in Table 1.

Cardiac geometry

Compared to normal fetuses, GDM fetuses demonstrated a significantly increased RV sphericity index and an increased thickness of IVS, LV and RV walls. There was a decreased LV end-diastolic dimension (EDD) and end-diastolic length (EDL) in GDM fetal group. Postnatally, in comparison to normal newborns, GDM neonates exhibited significantly increased RV/LV end-diastolic dimension ratio, RAVV/LAVV ratio and RV sphericity index, decreased LV EDD and EDL, and thickened IVS, LV and RV walls (Figure 1, Table 2). Perinatal geometrical changes from GDM fetuses to GDM neonates reflected a decrease in RV sphericity index, RV/LV end-diastolic dimension ratio and thickness of IVS and LV wall. The perinatal increase in both LV EDD and EDL in diabetic fetuses resulted in unchanged LV sphericity index (Figure 1, Table 2).

Global myocardial deformation and performance

Compared to normal controls, GDM fetuses had significantly higher values of longitudinal, circumferential and radial strain/systolic strain rate compared to normal fetuses, whereas GDM neonates showed significantly lower values of LV and RV longitudinal systolic strain rate, significantly higher LV basal radial strain rate, and increased both LV and RV MPI' (Figure 2, Table 2 and Table S1). Perinatal changes in the GDM group included a significant decrease in RV MPI', IVS longitudinal annular systolic motion and longitudinal, circumferential and radial strain/systolic strain rate (Table 2 and Table S1).

Systolic function

There were significant increases in myocardial annular systolic velocities S', LV ejection time' and RV isovolumetric contraction time' (IVCT'), and decreased LV cardiac output in GDM fetuses compared to normal fetuses. After birth, GDM neonates exhibited a significantly increased both LV and RV IVCT', decreased LV ejection, and similar values of LV and RV CO and heart rate compared to normal newborns (Table 2 and Table S1).

Perinatal changes in systolic function showed similar trends to those seen in a normal pregnancy with increased LV CO and a decrease in heart rate and RV IVCT' (Table 2).

Diastolic function

GDM fetuses had a significant decrease in IVS E'/A' ratio and a biventricular increase in isovolumetric relaxation time' (IVRT'). In the GDM neonate, there was a significant decrease in RV and LV diastolic inflow velocity ratio (RV $E/A < 1$ and LV $E/A > 1$), and diastolic LV E'/A' , IVS E'/A' and RV E'/A' ($E'/A' < 1$) ratios when compared to normal neonates. GDM newborns also revealed a significant increase in LV and RV E/E' ratios and LV and RV IVRT' (Table 2 and Table S1). Perinatal changes in GDM demonstrated a significant increase in LV and RV relaxation time periods and reduction of RV IVRT'. There was also a perinatal increased in LV E/A ratio ($E/A > 1$) and unchanged LV E'/A' ratio ($E'/A' < 1$) with a resulting increase in LV E/E' ratio (Table 2 and Table S1).

LV torsion

LV torsion values were significantly higher in GDM fetuses and neonates compared to normal controls (Figure 2 and Table S1). There were significant associations between LV torsion and multiple cardiac indices in fetuses and neonates (Figures 3). The fetuses with the highest values of LV torsion had indices reflecting increased cardiac systolic function. All neonates of women with pre-gestational insulin-dependent diabetes exhibited LV twist with the higher values of LV basal rotation compared to women with gestational diabetes mellitus (Figure S1).

Summary of alterations in cardiac parameters in GDM term fetus and neonates compared to normal groups presented in Table 3 and Figure 4. The limits of agreement (LoA) and intra-class correlation coefficient (ICC) showed excellent intra- and inter-observer agreement of all fetal and neonatal TDI and STI indices (ICC=0.8-0.9). Radial deformation showed moderate correlation and excellent agreement (Table S2).

DISCUSSION

Our study presents a comprehensive paired analysis of cardiac geometric and functional parameters in GDM fetuses and neonates. The findings show that GDM fetuses exhibit profound alterations in cardiac geometry, myocardial deformation and ventricular function, with evidence of persistence of some of these alterations after birth. These observations are likely to be responses to a relatively hyperglycemic intrauterine environment in gestational diabetes and adaptation to changes in volume and resistance loading conditions at birth.

Fetal cardiac geometry and function

GDM fetuses had a shorter and narrower left ventricle resulting in the same LV sphericity index as in normal fetuses. In contrast, the RV sphericity index was increased due to a shorter right ventricle length along with thickening of the IVS, LV and RV walls. The increased thickness of ventricular walls and ventricular hypertrophy has been reported previously with maternal diabetes and attributed to the altered metabolic environment and fetal hyperinsulinemia (3, 17). Recent animal studies implicated adverse cardiac remodelling, including dysregulation of the growth factors (IGF1 and IGF2), elevated collagen synthesis, profibrosis, and apoptosis as the aetiology of fetal cardiac hypertrophy, ventricular chamber dilatation and myocardial dysfunction in gestational diabetes (18, 19). Previous studies reported that increased contractility in GDM fetuses is a compensatory mechanism to fetal hypoxemia (20) which after a finite period of time could lead to an increased ventricular wall stress resulting in a myocardial cell damage, myocyte death and local fibrosis (21).

Consistent with this process, we found increased circumferential and radial myocardial deformation, higher LV torsion, longer LV IVRT and decreased IVS E' / A' ratio as well as

lower LV cardiac output in GDM fetuses indicative of myocardial impairment and ventricular dysfunction (22, 23). Our results suggest that despite compensatory increased systolic contractility and LV ejection time, a stiffer hypertrophied left ventricle in GDM fetuses might be responsible for a limited LV preload and a decreased LV chamber dimensions that may explain a significantly low LV CO observed in GDM term fetuses. In contrast, the right ventricle in the diabetic fetus has to work against an additional increase in afterload under conditions of hypoxemia. Although the right ventricle in GDM term fetuses exhibited a significantly increased longitudinal contractility, the known afterload sensitivity might limit the ability of the right ventricle to increase the cardiac output above the normal values and could contribute to RV chamber thickening and dilatation with signs of systolic and diastolic dysfunction evident from a prolonged RV IVCT' and IVRT' intervals.

Neonatal cardiac geometry and function

There were persistent alterations in the LV chamber geometry with thicker walls and narrower and shorter ventricles in neonates of diabetic mothers. GDM newborns showed a persistent increase in RV sphericity index resulting from an increased RV end-diastolic dimensions and a decrease in RV length, and thicker ventricular walls indicative of a more globular and thickened chamber. Presence of mild tricuspid regurgitation in the majority of GDM newborns might reflect persistently elevated pulmonary artery pressure that increases RV afterload, while tricuspid regurgitation could also add to RV volume load. These factors could contribute to persistent RV chamber enlargement and globular shape observed in the proportion of GDM neonates in our study. Impaired myocardial performance in GDM neonates was evident from our findings of significantly decreased biventricular longitudinal systolic contractility obtained by M-mode, PW-TDI and speckle tracking techniques. As longitudinal fibres are the most sensitive to oxygen demands, these results could suggest of a

possible subendocardial microvascular ischemic changes previously reported in the diabetic heart (24). Additionally, our results showed increased biventricular IVCT and IVRT periods resulting in elevated LV and RV MPI', as well as from evidence of biventricular diastolic dysfunction ($E'/A' < 1$ and increased E/E' ratio) with significantly elevated LV torsion – as reflected by recent experimental murine studies (25, 26). Our findings are supported by studies demonstrating impaired diastolic function and increased LV torsion (11, 12) in neonates of diabetic mothers, and persistence of ventricular hypertrophy and diastolic dysfunction in GDM infants up to 3 months of age (4).

Perinatal cardiac changes

Significant perinatal changes included decreased RV sphericity index at the expense of an increase in RV length and indicative of a decrease in the RV preload postnatally. There was also a significant perinatal increase in LV end-diastolic dimensions and length resulting in unchanged LV sphericity. These geometric changes were associated with lower LV and RV longitudinal systolic deformation and higher apical radial deformation. These findings are similar to those that we previously observed in normal pregnancy (15) suggesting that the decrease in global myocardial deformation, RV MPI' and increase in LV cardiac output are a consequence of the increase in LV and decrease in RV loading that occurs at birth. However, there was an unchanged LV MPI' due to persistently prolonged both IVCT' and IVRT'. The lack of perinatal increase in RV and LV E/A and E'/A' ratios and a significant increase in LV E/E' ratio, are indicative of persistence of RV and LV diastolic dysfunction in the first few hours after birth.

Strengths and limitations

The main strength of the present study was its prospective follow-up design and the inclusion of a healthy and pathological (GDM) study population where the impact of birth - a natural intervention - was studied longitudinally. Strict methodology and the same manner of fetal and neonatal cardiac assessment confirmed by good intra- and inter-observer repeatability insured the plausibility of our findings. The limitation of our study was a proportionately small number of GDM pregnancies (n=21) which included both gestational and pre-gestational diabetic patients under different treatments (insulin and metformin); however, the study power was sufficient to demonstrate significant alterations in cardiac parameters between study groups.

Conclusions

Gestational diabetes term fetuses and neonates exhibit altered cardiac indices indicative of myocardial impairment and ventricular dysfunction that are likely to reflect responses to changes in loading conditions occurring around the time of birth, presumably secondary to the metabolic derangement, hyperinsulinemia and relative fetal hypoxemia. Improvement in some of these cardiac indices in GDM neonates reflective of acute perinatal changes in haemodynamic load. Evidence of persistent alterations in ventricular geometry and function in the first days after birth could signal a predisposition to long-term cardiovascular morbidity in GDM offspring and merit further investigation in a prospective follow up study of these neonates in later childhood. It would be of great interest to assess whether these geometrical and functional alterations persist through infancy and the long-term outcome of our study neonates in later childhood. The study findings may be of relevance in optimising the perinatal outcomes of GDM pregnancy using the fetal period as a potential window for future interventions.

ACKNOWLEDGEMENT

We are grateful to all patients that have taken part in this study. We also thank General Electric Ultrasound Company for providing ultrasound platform and software for this research, Dr Margarita Bartsota and Miss Vahideh Davatgar Zahiri for helping with reproducibility study measurements, and all sonographers, midwives and doctors of the Fetal Medicine Unit, St. George's Hospital for their contribution to study patient recruitment.

CONFLICT OF INTERESTS

The authors report no conflict of interest.

FUNDING SOURCES

OP was partly supported by Children's Heart Unit Fund (CHUF), Royal Brompton and Harefield Hospital Charity [registration number 1053584] and SPARKS charity (registered no.1003825, grant ref. no.14EDI01).

REFERENCES

1. Mathiesen ER, Ringholm L, Damm P. Stillbirth in diabetic pregnancies. *Best Pract Res Clin Obstet Gynaecol.* 2011; **25**: 105-111.
2. Pedersen J. Diabetes and pregnancy; blood sugar of newborn infants during fasting and glucose administration. *Nord Med.* 1952; **47**: 1049.
3. Garg S, Sharma P, Sharma D, Behera V, Durairaj M, Dhall A. Use of fetal echocardiography for characterization of fetal cardiac structure in women with normal pregnancies and gestational diabetes mellitus. *J Ultrasound Med.* 2014; **33**: 1365-1369.
4. Arslan D, Oran B, Vatansev H, Cimen D, Guvenc O. The usefulness of plasma asymmetric dimethylarginine (ADMA) levels and tissue doppler echocardiography for heart function in term infants born to mothers with gestational diabetes mellitus. *J Matern Fetal Neonatal Med.* 2013; **26**: 1742-1748.
5. Marco LJ, McCloskey K, Vuillermin PJ, Burgner D, Said J, Ponsonby AL. Cardiovascular disease risk in the offspring of diabetic women: the impact of the intrauterine environment. *Exp Diabetes Res.* 2012; **2012**: 565160.
6. Comas M, Crispi F, Cruz-Martinez R, Martinez JM, Figueras F, Gratacos E. Usefulness of myocardial tissue Doppler vs conventional echocardiography in the evaluation of cardiac dysfunction in early-onset intrauterine growth restriction. *Am J Obstet Gynecol.* 2010; **203**: 45 e41-47.
7. Crispi F, Bijns B, Sepulveda-Swatson E, Cruz-Lemini M, Rojas-Benavente J, Gonzalez-Tendero A, Garcia-Posada R, Rodriguez-Lopez M, Demicheva E, Sitges M, Gratacos E. Postsystolic shortening by myocardial deformation imaging as a sign of cardiac adaptation to pressure overload in fetal growth restriction. *Circ Cardiovasc Imaging.* 2014; **7**: 781-787.

8. Wang X, Lian Y, Wang X, Tian M. Study of Regional Left Ventricular Longitudinal Function in Fetuses with Gestational Diabetes Mellitus by Velocity Vector Imaging. *Echocardiography*. 2016; **33**: 1228-1233.
9. Kulkarni A, Li L, Craft M, Nanda M, Lorenzo JM, Danford D, Kutty S. Fetal Myocardial Deformation in Maternal Diabetes Mellitus and Obesity. *Ultrasound Obstet Gynecol*. 2017; **49(5)**: 630-636.
10. Miranda JO, Cerqueira RJ, Ramalho C, Areias JC, Henriques-Coelho T. Fetal Cardiac Function in Maternal Diabetes: A Conventional and Speckle-Tracking Echocardiographic Study. *J Am Soc Echocardiogr*. 2018; **31(3)**:333-341.
11. Liao WQ, Zhou HY, Chen GC, Zou M, Lv X. [Left ventricular function in newborn infants of mothers with gestational diabetes mellitus]. *Zhongguo Dang Dai Er Ke Za Zhi*. 2012; **14**: 575-577.
12. Al-Biltagi M, Tolba OA, Rowisha MA, Mahfouz Ael S, Elewa MA. Speckle tracking and myocardial tissue imaging in infant of diabetic mother with gestational and pregestational diabetes. *Pediatr Cardiol*. 2015; **36**: 445-453.
13. NICE. National Institute for Health and Care Excellence (NICE) Diabetes in pregnancy: management from preconception to the postnatal period: NICE Guideline [NG3]. London: NICE. 2015.
14. Rodriguez-Lopez M, Cruz-Lemini M, Valenzuela-Alcaraz B, Garcia-Otero L, Sitges M, Bijns B, Gratacos E, Crispi F. Descriptive analysis of the different phenotypes of cardiac remodeling in fetal growth restriction. *Ultrasound Obstet Gynecol*. 2016.
15. Patey O, Gatzoulis MA, Thilaganathan B, Carvalho JS. Perinatal Changes in Fetal Ventricular Geometry, Myocardial Performance, and Cardiac Function in Normal Term Pregnancies. *J Am Soc Echocardiogr*. 2017; **30**: 485-492.e485.

16. Patey O, Carvalho, J.S., Thilaganathan, B. Perinatal changes in cardiac geometry and function in growth restricted fetuses at term. *Ultrasound Obstet Gynecol* 2018
17. Chu C, Gui YH, Ren YY, Shi LY. The impacts of maternal gestational diabetes mellitus (GDM) on fetal hearts. *Biomed Environ Sci.* 2012; **25**: 15-22.
18. Lehtoranta L, Vuolteenaho O, Laine VJ, Koskinen A, Soukka H, Kyto V, Maatta J, Haapsamo M, Ekholm E, Rasanen J. Maternal hyperglycemia leads to fetal cardiac hyperplasia and dysfunction in a rat model. *Am J Physiol Endocrinol Metab.* 2013; **305**: E611-619.
19. Lin X, Yang P, Reece EA, Yang P. Pregestational type 2 diabetes mellitus induces cardiac hypertrophy in the murine embryo through cardiac remodeling and fibrosis. *Am J Obstet Gynecol.* 2017.
20. Escobar J, Teramo K, Stefanovic V, Andersson S, Asensi MA, Arduini A, Cubells E, Sastre J, Vento M. Amniotic fluid oxidative and nitrosative stress biomarkers correlate with fetal chronic hypoxia in diabetic pregnancies. *Neonatology.* 2013; **103**: 193-198.
21. Hauton D, Ousley V. Prenatal hypoxia induces increased cardiac contractility on a background of decreased capillary density. *BMC Cardiovasc Disord.* 2009; **9**: 1.
22. Ren Y, Zhou Q, Yan Y, Chu C, Gui Y, Li X. Characterization of fetal cardiac structure and function detected by echocardiography in women with normal pregnancy and gestational diabetes mellitus. *Prenat Diagn.* 2011; **31**: 459-465.
23. Hatem MA, Zielinsky P, Hatem DM, Nicoloso LH, Manica JL, Piccoli AL, Zanettini J, Oliveira V, Scarpa F, Petracco R. Assessment of diastolic ventricular function in fetuses of diabetic mothers using tissue Doppler. *Cardiol Young.* 2008; **18**: 297-302.
24. Law B, Fowlkes V, Goldsmith JG, Carver W, Goldsmith EC. Diabetes-induced alterations in the extracellular matrix and their impact on myocardial function. *Microsc Microanal.* 2012; **18**: 22-34.

25. Laustsen PG, Russell SJ, Cui L, Entingh-Pearsall A, Holzenberger M, Liao R, Kahn CR. Essential role of insulin and insulin-like growth factor 1 receptor signaling in cardiac development and function. *Mol Cell Biol.* 2007; **27**: 1649-1664.
26. Lehtoranta L, Vuolteenaho O, Laine J, Polari L, Ekholm E, Rasanen J. Placental structural abnormalities have detrimental hemodynamic consequences in a rat model of maternal hyperglycemia. *Placenta.* 2016; **44**: 54-60.

Table 1 Demographic characteristic of the study population

Parameter	Normal (n=54)	GDM (n=21)	p- value
<i>Maternal characteristics</i>			
Maternal age (years)	33 ± 5	34 ± 6	0.892
Ethnicity (number): Caucasian	35 (65%)	5 (24%)	0.002
Asian	15 (28%)	12 (57%)	
Afro-Caribbean	4 (7%)	4 (19%)	
Delivery mode (C-section) (number)	14 (26%)	15 (71%)	0.002
Gestational age at delivery (weeks)	40 (0.2)	39 (0.8)	0.461
<i>Fetal assessment</i>			
Gestational age (weeks)	38 (3)	38 (1)	0.182
Time gap between the fetal scan and birth (days)	10 (7)	10 (5)	0.567
<i>Neonatal assessment</i>			
Neonatal age at the time of scan (days)	0.0 (0.5)	0.3 (0.9)	0.075
Neonatal sex (male, number)	28 (52%)	9 (43%)	0.664
Neonatal weight (kilograms)	3.514 ± 0.440	3.495 ± 0.601	0.907
Neonatal length (centimetres)	53.5 ± 3.7	50.9 (4.3)	0.185
Patent foramen ovale (number)	54 (100%)	21 (100%)	0.833
Patent ductus arteriosus (number)	32 (59%)	18 (86%)	0.705
<i>Pregnancy outcome</i>			
Tricuspid regurgitation (number)	3 (6%)	10 (48%)	<0.001
Admission to NICU (number)	0 (0%)	2 (11%)	0.235

Values are mean \pm SD, median (interquartile range), or n (%); GDM, gestational diabetes mellitus; NICU, neonatal intensive care unit.

Table 2 Perinatal changes in cardiac geometry and function in GDM term fetuses and neonates compared to normal controls

Parameters	Fetus at term		Neonate	
	Normal	GDM	Normal	GDM
<i>Cardiac geometry</i>				
RAVV/LAVV ratio	1.18 (0.21)	1.20 (0.33)	0.97 (0.08)	1.17 (0.15)*
LV EDL, mm	29.3 ± 5.0	26.1 ± 3.9†	33.7 ± 3.3	30.5 ± 3.6*§
RV EDL, mm	30.3 (6.8)	24.0 (4.6)*	32.2 ± 3.3	28.8 ± 4.0*§
LV EDD, mm	14.1 ± 2.1	12.7 ± 1.8†	16.8 ± 1.7	15.2 ± 1.3*‡
RV EDD, mm	16.8 ± 1.8	16.2 ± 1.9	13.9 ± 1.5	15.5 ± 1.3*
RV/LV EDD ratio	1.2 (0.2)	1.2 (0.3)	0.9 (0.1)	1.0 (0.1)*§
LV sphericity index	0.49 ± 0.09	0.49 ± 0.08	0.50 ± 0.09	0.50 ± 0.05
RV sphericity index	0.56 ± 0.09	0.65 ± 0.11†	0.43 ± 0.05	0.55 ± 0.08*§
Relative IVS thickness	0.77 ± 0.27	1.23 ± 0.39*	0.49 ± 0.14	0.71 ± 0.27*§
Relative LV wall thickness	0.77 ± 0.24	1.31 ± 0.27*	0.54 ± 0.13	0.75 ± 0.28†§
Relative RV wall thickness	0.62 ± 0.12	0.99 ± 0.28*	0.60 ± 0.16	1.01 ± 0.38*
<i>Global myocardial performance</i>				
LV MPI'	0.52 (0.14)	0.53 (0.11)	0.39 (0.11)	0.51 (0.15)*
RV MPI'	0.52 (0.13)	0.50 (0.14)	0.34 (0.06)	0.40 (0.07)†‡
<i>Systolic function</i>				
Heart rate, bpm	137 ± 10	140 ± 9	115 (18)	117 (9)‡
LV CO, ml/min/kg	197 (75)	136 (45)†	270 ± 59	254 ± 38‡
RV CO, ml/min/kg	213 (73)	251 (10)	208 (68)	217 (64)

IVS S', cm/s	0.14 (0.18)	0.17 (9.03)†	0.14 (0.05)	0.16 (0.04)†
RV S', cm/s	0.18 (0.10)	0.28 (0.06)*	0.20 (0.08)	0.22 (0.07)
LV IVCT', ms	107 ± 18	108 ± 23	78 ± 14	105 ± 97*
RV IVCT', ms	107 (33)	119 (37)*	70 (19)	84 (9)*§
Diastolic function				
LV E'/A'	0.77 (0.24)	0.60 (0.22)*	1.23 (0.27)	0.79 (0.39)*
LV E/E'	7.07 (2.14)	8.20 (3.17)	8.79 (3.36)	11.12 (5.01)*‡
IVS E'/A'	0.71 (0.14)	0.60 (0.19)*	1.00 (0.4)	0.75 (0.12)*
RV E'/A'	0.72 (0.30)	0.68 (0.17)	0.72 (0.39)	0.64 (0.24)†
RV E/E'	9.10 (3.97)	8.24 (2.45)	6.64 ± 1.45	7.90 ± 2.21†
LV IVRT', ms	101 ± 19	115 ± 21†	78 ± 17	103 ± 19*
RV IVRT', ms	107 ± 15	116 ± 21†	71 ± 12	90 ± 15*§

Values are mean ± SD, median (interquartile range). GDM, gestational diabetes mellitus; LV, left ventricular; RV, right ventricular; IVS, interventricular septal; RAVV = right atrioventricular valve; LAVV = left atrioventricular valve; EDD, end-diastolic dimension; EDL, end-diastolic length; MPI', myocardial performance index derived by PW-tissue Doppler imaging; CO, cardiac output; E'/A', early diastolic myocardial velocity to late atrial contraction myocardial velocity ratio derived by PW-TDI technique; E/E', transvalvular early diastolic velocity to myocardial early diastolic velocity ratio; IVCT', isovolumetric contraction time obtained by PW-TDI; IVRT', isovolumetric relaxation time obtained by PW-TDI. *Sphericity index* = EDD/EDL. *Relative wall thickness* = (2 x wall thickness)/EDD. Time-intervals are normalised by cardiac cycle length, longitudinal systolic velocities S' were normalised by LV EDL. *, p-value < 0.001 and †, p-value <0.01 compared GDM fetuses and neonates with normal groups; ‡, p-values < 0.001 and §, p-value <0.01 compared GDM fetus with GDM neonate.

Table 3 Summary of alterations in cardiac parameters in GDM term fetus and neonates compared to normal groups

Cardiac geometry	Myocardial performance	Systolic function	Diastolic function
<i>GDM term fetuses compared to Normal fetuses</i>			
↑RV SI (shorter RV) ↓LV EDD and EDL (narrower and shorter LV) ↑ LV, RV and IVS thickness	↑LV _{basal} C-S and C-SR ↑LV _{basal} R-SR ↑LV L-S and L-SR ↑RV L-S and L-SR ↑LV torsion	↓LV CO ↑LV, IVS and RV S' ↑LV ET' ↑RV IVCT'	↑LV IVRT' ↑RV IVRT' ↓IVS E'/A' (<1)
<i>GDM neonates compared to Normal neonates</i>			
↑RV SI (wider and shorter RV) ↓LV EDD and EDL (narrower and shorter LV) ↑ LV, RV and IVS thickness	↓LV L-SR ↓RV L-S and L-SR ↑LV _{basal} R-SR ↑LV torsion ↑LV MPI' ↑RV MPI'	↓LV ET' ↑LV IVCT' ↑RV IVCT'	↑LV IVRT' ↑RV IVRT' ↓LV E'/A' (<1) ↓RV E'/A' (<1) ↑LV E/E' ↑RV E/E'

GDM, gestational diabetes mellitus; LV, left ventricular; RV, right ventricular; IVS, interventricular septal; EDD, end-diastolic dimension; EDL, end-diastolic length; SI, sphericity index; S, strain; SR, strain rate; L-SR, longitudinal strain rate; C-S, circumferential strain; C-SR, circumferential strain rate; R-S, radial strain; R-SR, radial strain rate; CO, cardiac output; S', systolic myocardial velocity; E/A, transvalvular early diastolic velocity to late atrial contraction velocity ratio obtained by PW Doppler; E'/A', early diastolic myocardial velocity to late atrial contraction myocardial velocity ratio derived by PW-TDI technique; E/E', transvalvular early diastolic velocity to myocardial early diastolic velocity ratio; IVCT', isovolumetric contraction time by PW-TDI; IVRT', isovolumetric relaxation time by PW-TDI; ↑, increased; ↓, decreased.

FIGURE LEGENDS

Figure 1 Cardiac geometry in GDM and normal term fetuses and neonates. Box-and-whisker plots demonstrate significant alterations in RV sphericity index in GDM groups compared to normal controls (normal fetuses and neonates are shown in *white*, GDM groups are in *black*); Boxes represent median and interquartile range, and whiskers are 5th and 95th centiles; Sphericity index = ventricular end-diastolic dimension/end-diastolic length; *, p-value < 0.001 and †, p-value < 0.01.

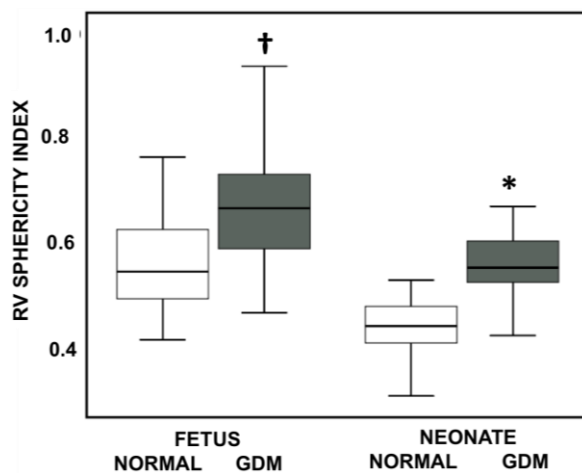


Figure 1.

Figure 2 Myocardial deformational parameters in normal and GDM term fetuses and neonates. Speckle tracking myocardial deformational curve showing the systolic peaks of RV longitudinal strain [L-S] (A) and LV apical circumferential strain [C-S] (B) in GDM term fetus. Box-and-whisker plots demonstrate LV basal radial strain rate [R-SR] (C) and LV torsion (D) in GDM fetus and neonates compared to normal groups (normal fetuses and neonates are shown in *white*, and GDM groups are in *black* colour); Boxes represent median

and interquartile range, and whiskers are 5th and 95th centiles; *, p-value < 0.001 and †, p-value < 0.01.

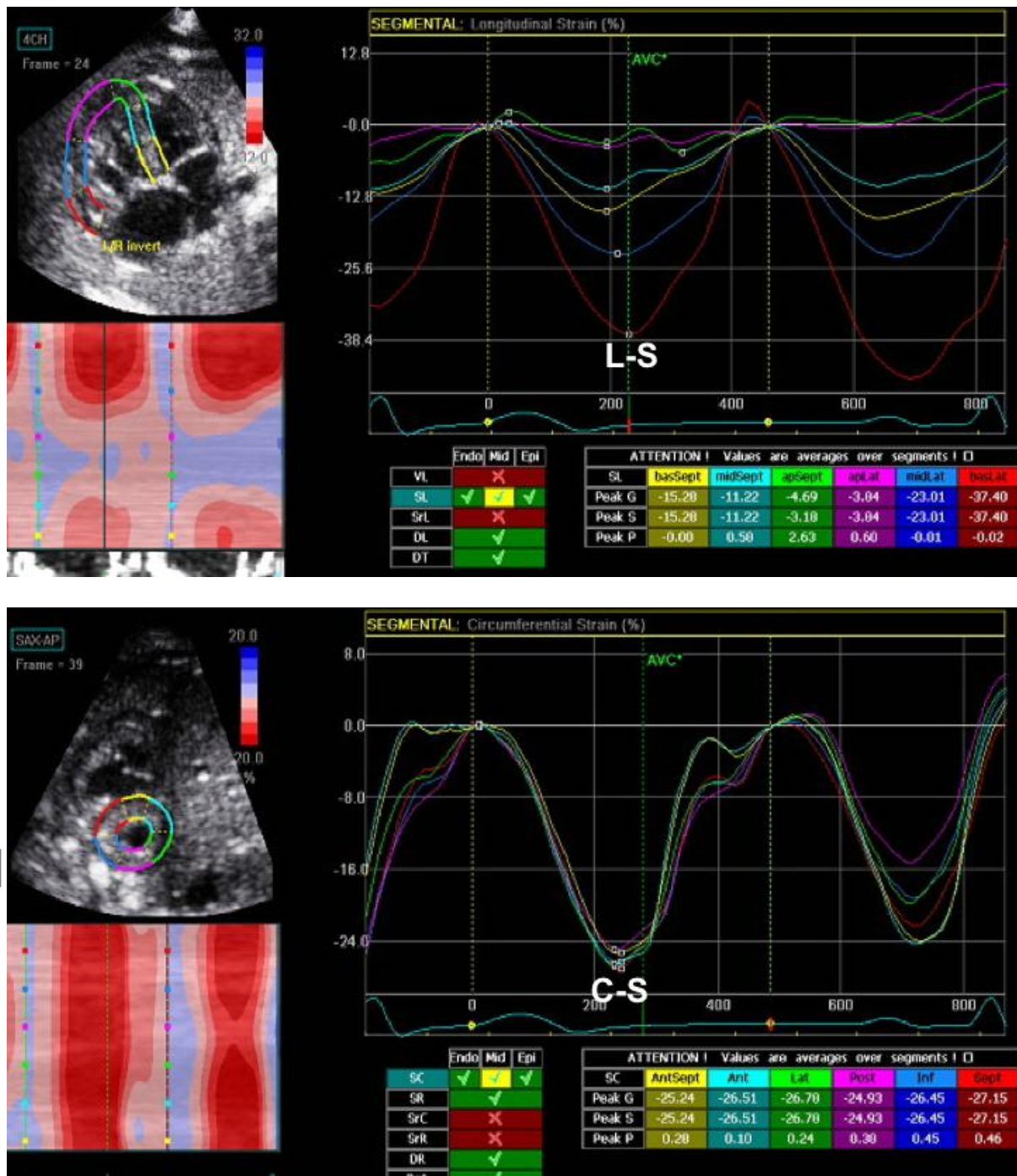
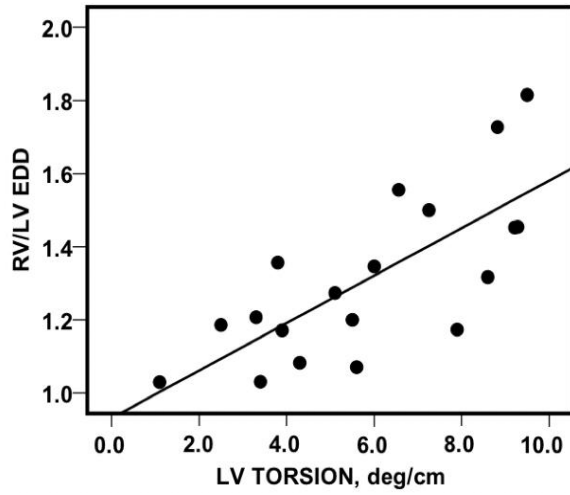
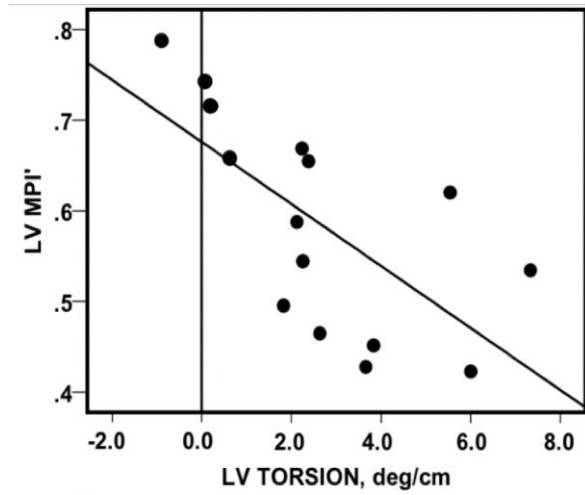


Figure 3 Linear correlation of LV rotational indices with other cardiac parameters in GDM fetuses and neonates. Scatter plots showing a significant linear correlation of an increased LV torsion with an increased RV/LV end-diastolic ratio [EDD] in GDM fetus

($R^2=0.52$, $p=0.001$) (A), and a decreased LV myocardial performance index [MPI'] in GDM neonate ($R^2= 0.66$, $p=0.006$) (B).



A.



B.

Figure 3.

Figure 4 Summary of cardiac geometrical and functional alterations in GDM fetuses and neonates compared to normal controls. Spiderweb plot showing significant alterations of cardiac parameters in GDM term fetuses (*blue*) and GDM neonates (*red*) compared to normal controls (*green*). IVS, interventricular septum; LV, left ventricular; RV, right ventricular; SI, sphericity index; L-SR, longitudinal strain rate; R-SR, radial strain rate; CO, cardiac output; IVCT', isovolumetric contraction time; IVRT', isovolumetric relaxation time.

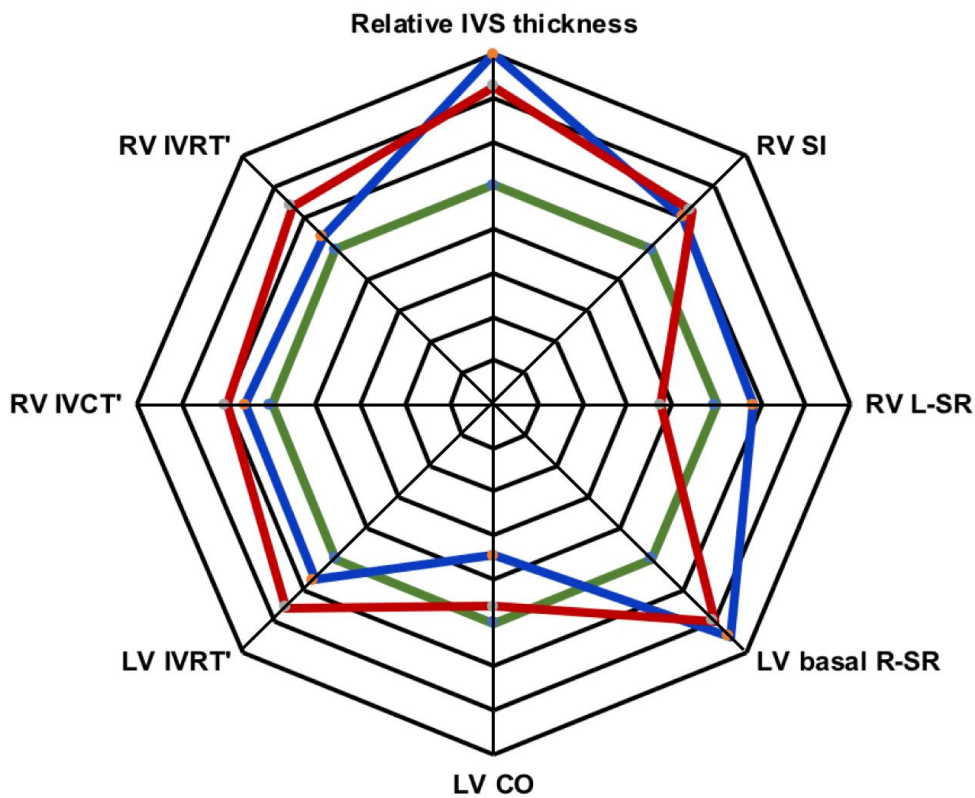


Figure 4.